



Pergamon

Materials Research Bulletin 36 (2001) 755–765

Materials
Research
Bulletin

Novel synthesis of high phase-purity Mg_2SnO_4 from metallic precursors via powder metallurgy route

Abdul-Majeed Azad^{1,*}

Advanced Materials Research Center, SIRIM Berhad, PO Box 7035, 40911 Shah Alam, Selangor, Malaysia

(Refereed)

Received 24 July 2000; accepted 7 September 2000

Abstract

A novel yet simple technique of synthesizing oxide ceramics from metallic precursors has been described. Magnesium orthostannate, Mg_2SnO_4 , a potential candidate for applications in high temperature-high frequency domain as a ceramic capacitor element, was synthesized from metallic tin and magnesium powders. An alloy of composition Mg_2Sn was prepared by the conventional powder metallurgy route. This up on heating in air under carefully designed ordinary and mild experimental conditions, yielded single-phase inverse spinel type Mg_2SnO_4 . The systematic evolution of phase(s) and powder morphology of the target oxide is discussed and compared with those in powders obtained by other techniques. The present method totally obviates the use of resilient oxides and of carbonate and nitrates precursors, which are invariably the source of environmental pollutants such as CO_2 and NO_x . In addition, the difficulties normally encountered in ceramic syntheses from the significant difference in particle size of the starting powders are also eliminated. The technique offers an environmental-friendly viable solution to making dense ceramics in thin multilayer formats (MLFs) with miniaturized dimensions, provided a suitable metallic alloy precursor can be found in the relevant binary/ternary phase diagram. © 2001 Elsevier Science Ltd. All rights reserved.

Keywords: A. Alloys; A. Ceramics; A. Electronic materials; C. X-ray diffraction; D. Microstructure

1. Introduction

With an ever-increasing global emphasis on ‘green’ techniques for materials synthesis and device fabrication conforming to the environmental preservation and public health ethics,

* Corresponding author.

E-mail address: azad@nextechmaterials.com (A-M. Azad).

¹ Present address: NexTech Materials, Ltd., 720-I Lakeview Plaza Boulevard, Worthington, OH 43085, USA.

newer and environmentally safer methods ought to be devised. This is more relevant to the pharmaceutical and chemical industry that either use precursors or vent materials (as their byproducts) that are harmful to the environment and general public health. Various ceramic synthesis techniques also invariably end up in generating a great deal of harmful (solid/liquid/gas) wastes [1]. Development of advanced ceramics using numerous solution techniques (sol-gel, organometallic complexation, etc.) is a point in case. In addition, the conventional method of solid-state reaction between two or more precursors requires stages of repetitive performance, such as, several time-consuming steps of grinding, milling, heating, etc. [2]. This translates in many cases in higher energy consumption, long preparation time and on several occasions results in a product that would have inferior properties in the final composition. This aspect has been amply dealt with in a number of publications and monographs [2–8]. Thus, there is an urgent and genuine need to explore and develop newer and less energy intensive methods for advanced ceramics synthesis that are also environmentally benign.

The alkaline-earth stannates having the general chemical formula $M\text{SnO}_3$ ($M = \text{Ca}, \text{Sr}$ and Ba), and Mg_2SnO_4 have recently been studied as potential electronic ceramics, such as, thermally stable capacitors with low permittivity and small loss tangent for applications in high temperature-high frequency domain [9–24]. A number of techniques for materials synthesis, such as the conventional solid-state reaction, self-heat-sustained reaction, organometallic citrate complexation and sol-gel were employed in the above mentioned MO-SnO_2 systems. Systematic investigations with emphasis on material synthesis, phase relationship, microstructural features and the electrical characteristics of the sintered bodies have also been carried out. Interestingly, the behavior of magnesium metastannate (MgSnO_3) and orthostannate (Mg_2SnO_4) is totally different from the corresponding Ca, Sr and Ba counterparts. The meta- and orthostannates of calcium, strontium and barium are known to be stable independently up to very high temperatures without degradation. MgSnO_3 is unstable and disproportionates into orthostannate and tin oxide upon heating above $\sim 700^\circ\text{C}$. In some cases, even the orthostannate cannot be synthesized as a single-phase [25].

With an aim to: (i) obviate the use of traditional inorganic and/or organometallic precursors, (ii) minimize/eliminate the emission of obnoxious gaseous pollutants and, (iii) synthesize the desired compound under simpler and less demanding conditions, a novel reaction path via a powder metallurgy route using metallic precursors, towards the formation of phase pure Mg_2SnO_4 has been investigated. The systematic phase and microstructural evolution, perhaps for the first time, resulting from the oxidation of a Mg-Sn intermetallic is reported here.

2. Experimental procedure

Metallic Sn (99.85% powder, lot # B19G22, -100 mesh) and Mg (99.8% powder, lot # C20123, -20 +100 mesh) from Alfa Aesar, USA, were used as the starting materials. Stoichiometric amounts of tin and magnesium metal powders were accurately weighed so as to give 50g batch of Mg_2Sn alloy. The two were mixed manually in an agate mortar and pestle for 30 minutes. The mixture was placed in a high purity recrystallized alumina boat

that was then positioned in the uniform temperature zone (UTZ) of a horizontal furnace equipped with a fully automated microprocessor-based temperature controller (ChinoTM, Japan). The furnace tube was flushed with argon gas to displace the ambient air within the furnace tube. The furnace was heated slowly in argon (gas flow rate $\sim 10 \text{ Lh}^{-1}$), first to 250°C and maintained for 1 h to facilitate the melting of tin ($T_{\text{m, Sn}} = 232^\circ\text{C}$). The temperature was then raised to and maintained for 2 h at 775°C . A rate of 5° per minute was used during the heating and cooling. Steady flow of argon gas throughout the experiment was ensured to avoid the oxidation of the alloy during preparation stage.

The alloy thus obtained had a rather hard crust (having the appearance of a frozen mass, with a typical bluish black metallic luster) and a porous interior. The material was extracted, crushed and pulverized to fine powder, and subjected to phase analysis using room temperature powder X-ray diffraction (Rigaku, Japan) with CuK_α radiation ($\lambda = 1.5406 \text{ \AA}$) in the range $10^\circ - 80^\circ$ (2θ) with a scan rate of 2°min^{-1} . Prior to oxidation, the alloy powder was sieved through a $25\text{-}\mu\text{m}$ mesh and pressed into discs of 12-mm diameter and about 1-mm thickness by uniaxial pressing in stainless steel dies at pressures not exceeding 40 MPa. These pellets were heated in ambient air at different temperatures between 500°C to 1200°C for soak-time ranging between 1 and 24 h. XRD signatures were collected after each oxidation stage, to follow the sequence of the phase evolution and to discern the reaction pathway leading to the formation of the targeted compound.

Microstructural features of the starting alloy powder as well as the oxidized mass were determined by using a JEOL-6400SM or Hitachi-2500S (Japan) scanning electron microscope (SEM). For this purpose, powder was dispersed in acetone and evenly sprayed on the glued surface of an aluminum stub. Polaron Coating Machine (UK) evaporated a uniform film (10 \AA to 30 \AA thick) of gold to avoid electrostatic charging during microscopic viewing. The Mg_2Sn precursor powder and the oxidized discs were stored in humidity-free bottles containing anhydrous CaCl_2 , unless required for X-ray analyses or microscopic viewing.

3. Results and discussion

The Mg-Sn binary system constitutes a fairly simple phase diagram. Beside a region of limited solid solubility at the Mg-rich end (0.0925 at. % Sn at 200°C ; 0.9424 at. % Sn at 400°C) it consists of a tin-rich eutectic (90.4 at. % Sn, triple point = 203.5°C), a magnesium-rich eutectic (11 at. % Sn, triple point = 561.2°C) and a solitary line compound Mg_2Sn (33.33 at. % Sn) melting congruently at 770.5°C [26–27]. The intermetallic Mg_2Sn crystallizes in a fluorite (face-centered cubic) structure. It was therefore, envisaged that the oxidation of the compound Mg_2Sn could result in the corresponding oxide, viz., Mg_2SnO_4 (cubic spinel) under rather mild conditions, thereby obviating the difficulties of conventional synthesis processes outlined above.

The XRD pattern of the alloy prepared at 775°C from metallic tin and magnesium is displayed in Fig. 1. Comparison with the standard cards shows all the major diffraction peaks belonging to the compound Mg_2Sn (JCPDS 7–0274) alone with metallic tin (JCPDS 4–0673) present in traces only. Very sharp and narrow diffraction peaks also signify the formation of the precursor in highly crystalline state with small crystallite size. The XRD

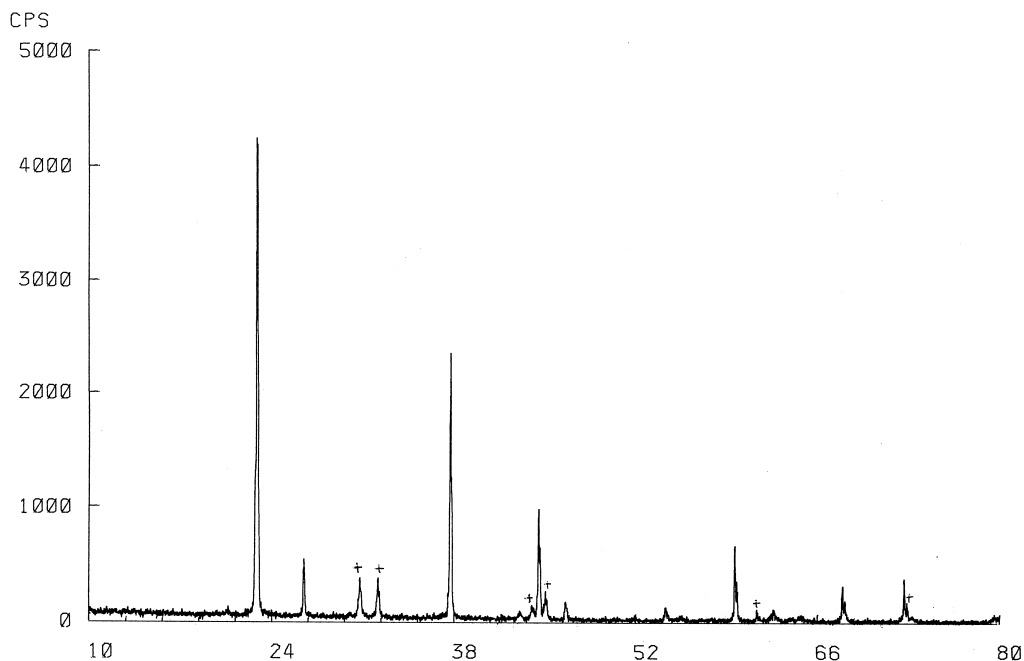


Fig. 1. X-ray diffractogram of Mg_2Sn prepared by powder metallurgy route. + = Sn.

pattern was used to compute the unit cell lattice parameter and crystal volume that yielded values of 6.7666×10^{-10} m and 309.82×10^{-30} m³ comparing well with the reported value of 6.7630×10^{-10} m and 309.33×10^{-30} m³ for the Mg_2Sn lattice edge and volume, respectively.

The powder morphology of the intermetallic phase is shown in Fig. 2, which has a typical chunky appearance of metallic systems. The powder consists mainly of agglomerates and aggregates that have large size distribution between a few microns to as much as 50 micron.

The alloy oxidation was carried out in a series of temperature-time (T-t) profiles listed in Table 1. Such a wide range of calcination schedule was employed to systematically follow the phase evolution at each stage and to unequivocally discern the reaction path leading to the formation of the target compound, Mg_2SnO_4 . As will be shown subsequently, up to certain temperatures the formation of the orthostannate was invariably accompanied by that of SnO_2 in a competitive fashion, the relative amounts of the two phases being strongly dependent on the heating profile. Fig. 3 shows the XRD signature acquired on the Mg_2Sn heated in air for 12 h at 500°C. The data analysis based on peak position revealed that at this stage the product consisted of a mixture of SnO_2 (JCPDS 41-1445) and MgO (JCPDS 4-0829) with small amounts of metallic Sn and Mg_2Sn as minor phases. There was no evidence of the double oxide formation. This was supported by the visual examination of the calcined matter that was grayish black in color; both $MgSnO_3$ and Mg_2SnO_4 are white. Thus, it appears that at 500°C the oxidation of the intermetallic into individual oxides is thermodynamically more feasible than the formation of the spinel phase directly.

Upon heating the intermetallic compound at 900°C for 1 h, characteristic peaks of magnesium orthostannate along with those for cassiterite were observed in the X-ray pattern.

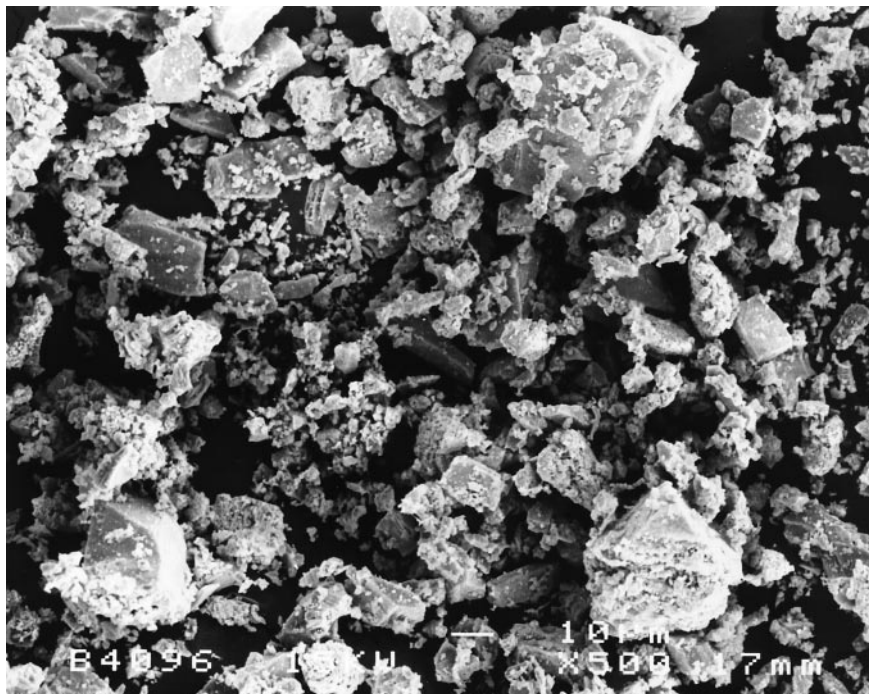


Fig. 2. Morphological features of Mg_2Sn powder.

The amount of spinel stannate steadily increased with a corresponding decrease in SnO_2 as the calcination time was increased from 1 h to 4 and 8 h. This could be clearly seen in Fig. 4 where the XRD signatures for 3 soak-times at 900°C are compared. It is obvious that as the time increased, the intensity of peaks corresponding to tin dioxide steadily decreased while those of the spinel phase showed an increasing trend. Samples subjected to oxidation experiments at 925°C for 4 to 24 h exhibited an identical trend albeit with even higher amount of Mg_2SnO_4 phase. The alloy powder calcined at 1200°C for 12 h resulted in a phase that was identified as high purity Mg_2SnO_4 with SnO_2 as a trace impurity. This is illustrated in Fig. 5 where the X-ray diffractograms of samples heated at $925^\circ\text{C}/24$ h and $1200^\circ\text{C}/12$ h

Table 1

Summary of the heat-treatment given to Mg_2Sn alloy to form Mg_2SnO_4

Temperature/ $^\circ\text{C}$	Soak-time/h	Heating rate ($^\circ/\text{min.}$)
500	12	1
900	1	5
	4	5
	8	5
	8	5
925	4	5
	8	5
	24	5
1200	12	10

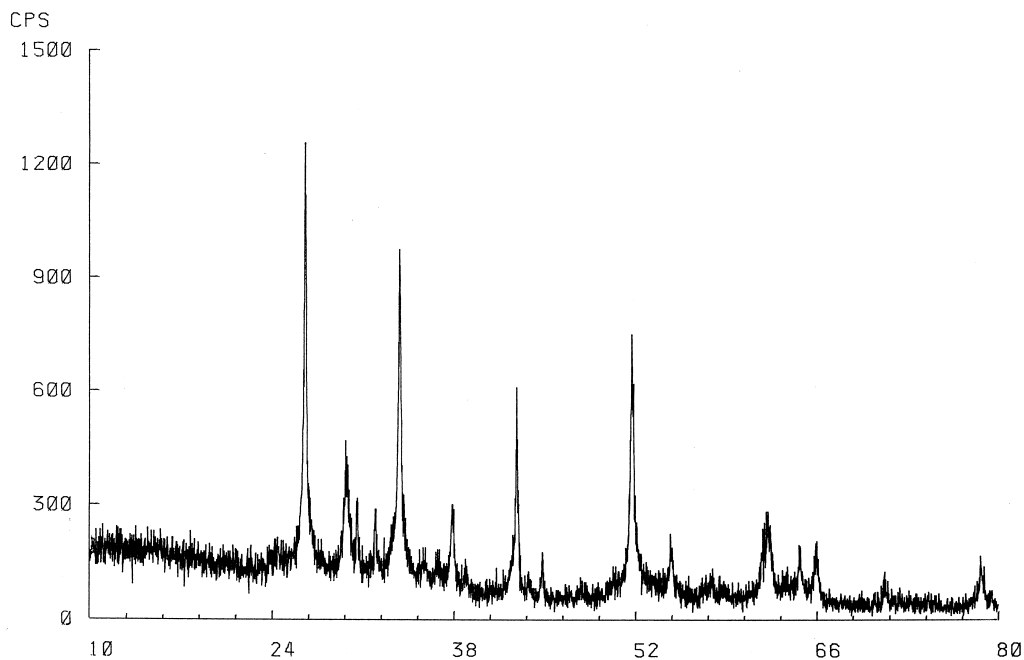


Fig. 3. Diffraction pattern of the Mg_2Sn sample subsequent to heating in air at $500^\circ C$ for 12 h.

are compared over the most significant 2θ range. A remarkable increase in the yield of the spinel phase and near non-existence of SnO_2 in samples heated at $1200^\circ C$ cannot be overlooked. The systematic variation in the relative amounts of magnesium orthostannate and tin oxide in the mixtures obtained upon calcination in the range $900\text{--}1200^\circ C$ for various

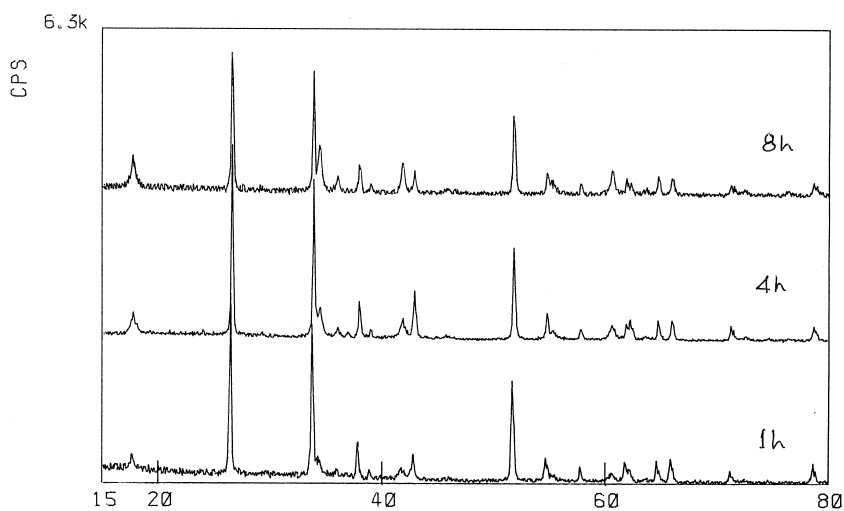


Fig. 4. XRD signatures showing the progress of phase evolution after Mg_2Sn is heated at $900^\circ C$ for 1, 4 and 8 h. Note the systematic increase in the intensity of Mg_2SnO_4 peaks at $\sim 17.8^\circ$ [111] and $\sim 34.4^\circ$ [311].

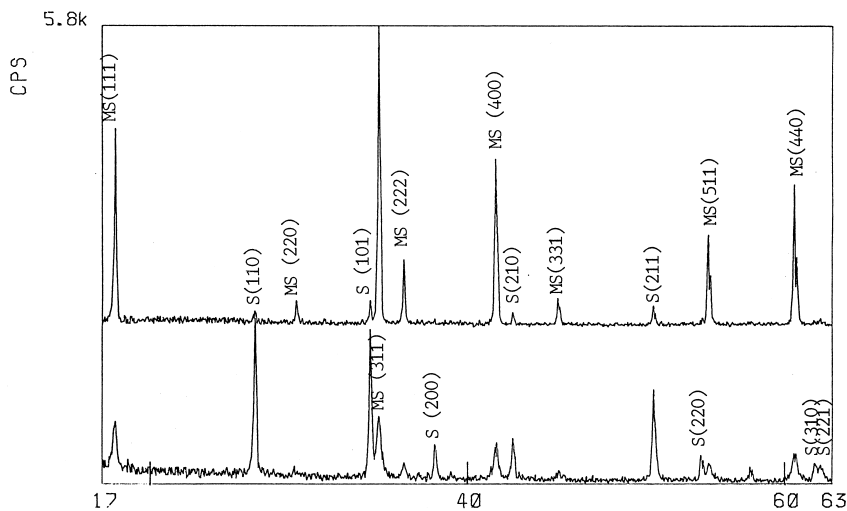


Fig. 5. Comparative XRD patterns of Mg_2Sn heated at $925^\circ C$ for 24 h and at $1200^\circ C$ for 12 h. S = SnO_2 , MS = Mg_2SnO_4 .

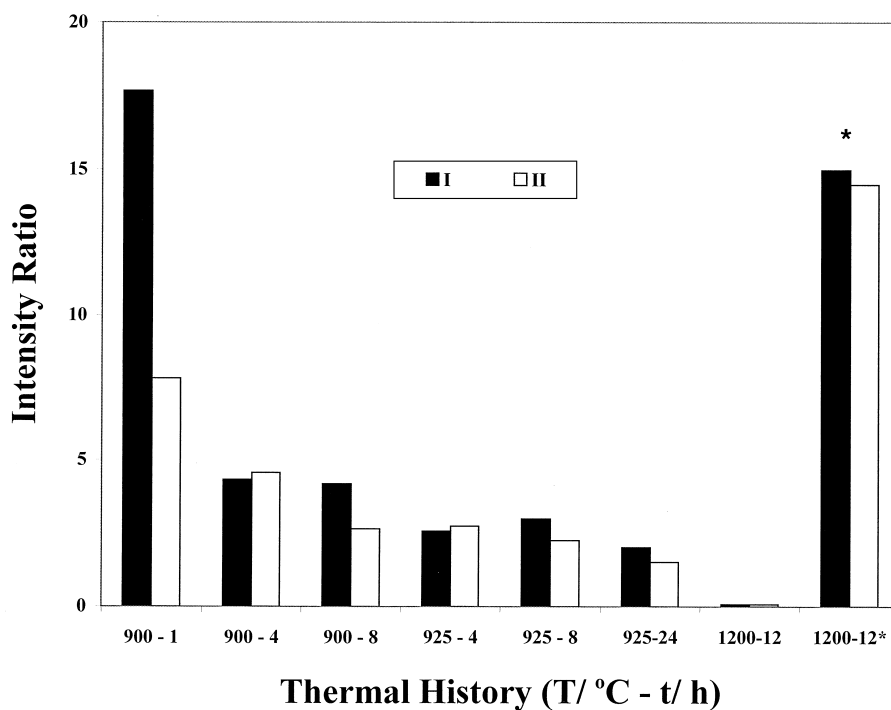


Fig. 6. Variation in the relative amounts of SnO_2 (S) and Mg_2SnO_4 (MS) formed up on Mg_2Sn oxidation under different conditions. I = S_{100}/MS_{111} ratio; II = S_{101}/MS_{311} ratio; * = MS/S ratio.

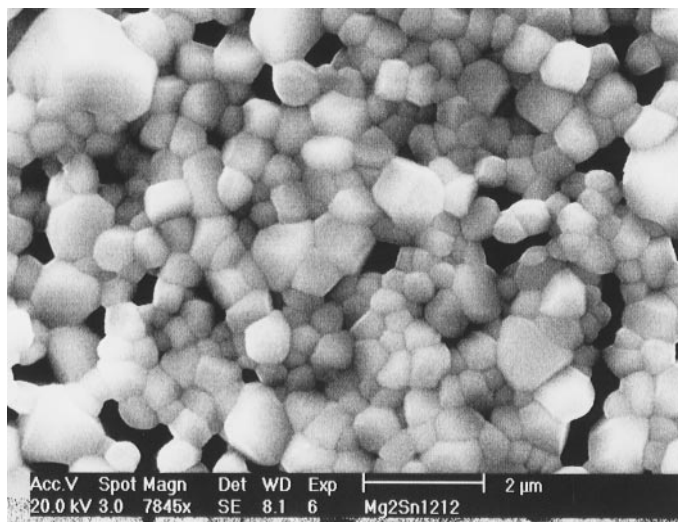


Fig. 7. SEM micrograph of the powder after Mg_2Sn oxidation at $1200^\circ\text{C}/12$ h.

duration, is shown in Fig. 6 in terms of the intensity ratio of the most prominent peaks corresponding to the two phases. For this purpose, heights of the diffraction peaks of [100] and [101] planes of SnO_2 were respectively compared with those of [111] and [311] planes belonging to Mg_2SnO_4 . It can be seen that, as the calcination temperature and time increased, Mg_2SnO_4 became more prominent with corresponding decrease in the amount of SnO_2 . This comparison clearly brings out the fact that a single-stage heating of Mg_2Sn at 1200°C for 12 h results in phase 'pure' Mg_2SnO_4 . The powder morphology presented in Fig. 7 shows highly angular crystallites with majority grains of sub-micron size. Estimation done by using Scherrer's equation [28]:

$$D = 0.9\lambda/\beta_{1/2} \cos\theta$$

where D = crystallite size

λ = wave length

$\beta_{1/2}$ = full width of the diffraction peak at half maximum and,

θ = angle of diffraction,

yielded a value of $\sim 0.4 \mu\text{m}$ for the average grain size. A typical EDAX spectrum is shown in Fig. 8. The EDAX analysis (by the standard less ZAF quantification method) done on agglomerates and several randomly chosen grains of this powder, shows the grain composition to be Mg_2SnO_4 . Values of 863.65 pm and $644.2 \times 10^{-30} \text{ m}^3$ computed from the diffractogram taken on samples calcined at 1200°C for 12 h compare well with the reported values of 863.76 pm and $644.4 \times 10^{-30} \text{ m}^3$ for the lattice parameter 'a' and unit cell volume, respectively for Mg_2SnO_4 [29].

At this juncture, it may be interesting to highlight the experimental conditions employed by others for the synthesis of Mg_2SnO_4 . Sample on which the reported XRD pattern (JCPDS card #24–0723) was generated, had been prepared by heating a 2:1 molar mixture of MgO and SnO_2 for 17 h at 1500°C , followed by regrinding and heating the powder again for 1 h

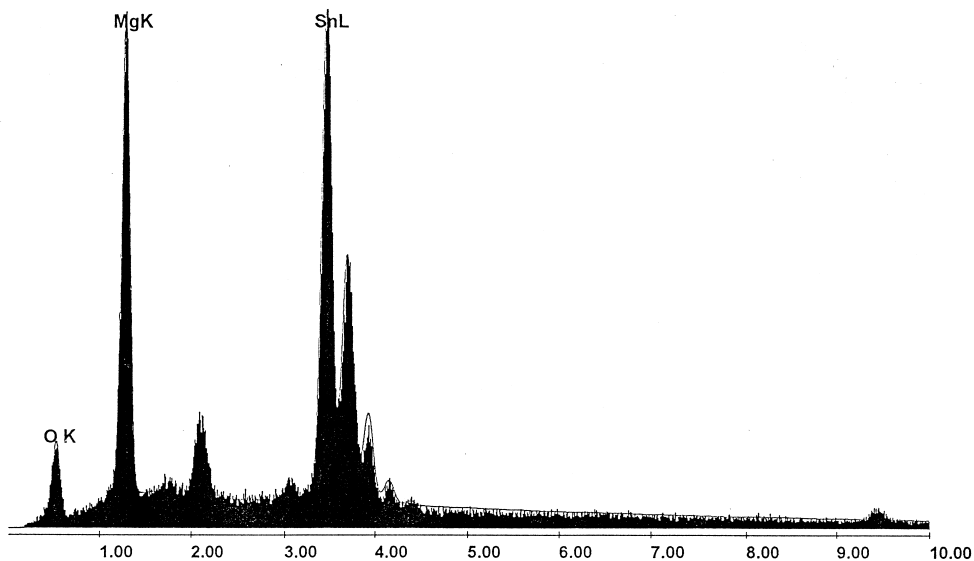


Fig. 8. A typical concentration profile of Mg, Sn and O by energy dispersive X-ray (EDX) analysis done on the powder subjected to oxidation at 1200°C/12 h.

at 1500°C [29]. Chang and Kaldon [30] reported the synthesis of magnesium orthostannate by heating the component oxides at 1100 °C for 400 h. Azad and Min [23,31] had recently employed magnesium nitrate and tin dioxide (2:1 molar mixtures) as the starting material for solid-state reaction synthesis. Their results showed that the final phase in powders obtained after a 2-step calcination at 1000°C and 1200°C for 12 h each, consisted predominantly of the orthostannate phase, viz., Mg_2SnO_4 , with some minor peaks corresponding to SnO_2 . In

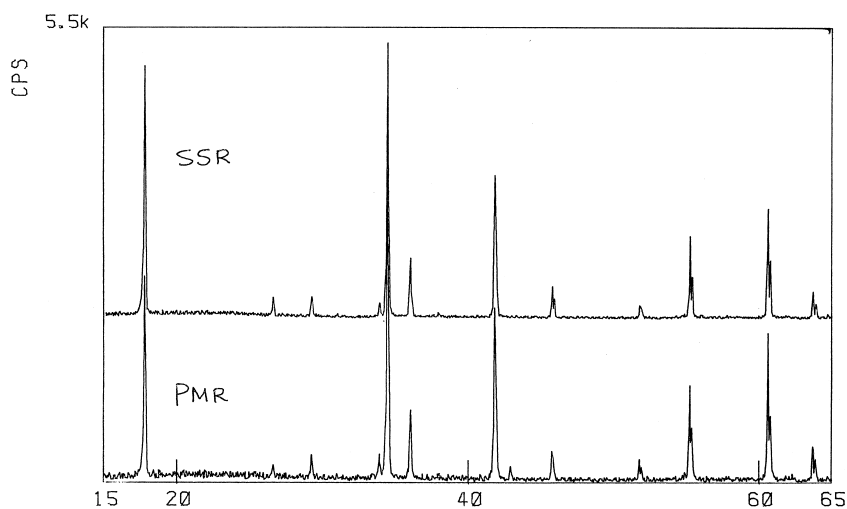


Fig. 9. Comparison of the XRD signatures of Mg_2SnO_4 prepared in this work with that from solid-state reaction between $\text{Mg}(\text{NO}_3)_2$ and SnO_2 .

powders prepared via the self-heat-sustained (SHS) technique employing magnesium nitrate and Sn metal, pure Mg_2SnO_4 was formed in mixtures calcined at 1300°C for 12 h. However, these powder compacts sintered at $1500^\circ\text{C}/6\text{ h}$ and $1600^\circ\text{C}/2\text{ h}$ led to pure Mg_2SnO_4 phase without even traces of other compound(s). Fig. 9 compares the X-ray diffractogram on powders derived from powder metallurgy route and solid-state reaction. Even though the quality of the end product obtained by the two methods is almost the same, the metallic precursor route investigated in this work has an edge over the conventional solid-state preparative technique, in that it obviates the stages of extensive ball milling, precalcination and the emission of gaseous byproducts. The production and subsequent oxidation of Mg_2Sn into Mg_2SnO_4 is attractive from the economy point of view as well; magnesium metal (\$1.53/lb.) is not as expensive as titanium (\$3.5 - \$4.5/lb.) or nickel (\$3.0/lb.) and is only twice as costly as aluminum (\$0.75/lb.) [32] and Mg_2Sn could be produced under very mild experimental conditions as was demonstrated in this work.

4. Conclusions

Synthesis of a potential electroceramic, viz., Mg_2SnO_4 via simple powder metallurgy route has been described. The method has definite advantages over the conventional solid-state reaction and many new and novel techniques of ceramic powder preparation. Phase pure compound has been obtained by the oxidation of a stoichiometric alloy under mild conditions. The powders thus obtained possessed rather small grain size, a narrow grain size distribution and exhibited lesser degree of agglomeration. As such the powder with these characteristics could be sintered to very high degree of densification without much elaborate prior processing. The method is applicable to many other binary/ternary metal-oxide systems, if intermetallics of the right stoichiometry can be found in the corresponding phase diagrams.

References

1. A.J. Cusumano, Chem. Edu. 72 (1995) 959.
2. W.D. Kingrey, H.K. Bowen, D.R. Uhlmann, Introduction to Ceramics, 2nd ed., John Wiley and Sons, New York, 1976.
3. R. Buchanan, Ceramic Materials for Electronics, Marcel Dekker, New York, 1986.
4. H. Schmalzried, Solid State Reactions, Verlag Chemie GmbH, Weinheim, 1981.
5. G.P. Binner, Advanced Ceramic Processing and Technology, vol. 1, Noyes Publication, New York, 1990.
6. A.J. Moulson, J.M. Herbert, Electroceramics. Materials, Processing, Applications, Chapman and Hall, New York, 1990.
7. J.M. Herbert, Ceramic Dielectrics and Capacitors, Gordon and Breach Science Publishers, Philadelphia, 1985.
8. H.J. Schmutzler, M.A. Anthony, K.H. Sandhage, J. Am. Ceram. Soc. 77 (1994) 721.
9. O. Parkash, K.D. Mandal, C.C. Christopher, M.S. Sastry, D. Kumar, J. Mater. Sci. Lett. 13 (1994) 1616.
10. K.D. Mandal, M.S. Sastry, O. Parkash, J. Mater. Sci. Lett. 14 (1995) 1412.
11. S. Upadhyay, O. Parkash, D. Kumar, J. Mater. Sci. Lett. 16 (1997) 1330.
12. M.G. Smith, J.B. Goodenough, A. Manthiram, R.D. Taylor, W. Peng, C.W. Kimball, J. Solid. State. Chem. 98 (1992) 181.

13. M. Bao, W.D. Li, P. Zhu, *J. Mater. Sci.* 28 (1993) 6617.
14. S. Upadhyay, A.K. Sahu, D. Kumar, O. Parkash, *J. Appl. Phys.* 84 (1998) 828.
15. C.P. Udawatte, M. Kakihana, M. Yoshimura, *Solid State Ionics* 108 (1998).23.
16. A.-M. Azad, in: M. A. Khan, A. Haq, K. Hussain, A. Q. Khan (Eds.), *Proceedings of the 5th International Symposium on Advanced Materials*, Dr. A. Q. Khan Research Laboratories, Kahuta, Pakistan, 1997, pp. 110–117.
17. A.-M. Azad, N.C. Hon, *J. Alloys. Comp.* 270 (1998) 95.
18. A.-M. Azad, L.L.W. Shyan, P.T. Yen, *J. Alloys. Comp.* 282 (1999) 109.
19. A.-M. Azad, L.L.W. Shyan, M.A. Alim, *J. Mater. Sci.* 34 (1999) 1175.
20. A.-M. Azad, L.L.W. Shyan, M.A. Alim, *J. Mater. Sci.* 34 (1999) 3375.
21. A.-M. Azad, L.L.W. Shyan, P.T. Yen, N.C. Hon, *Ceram. Int.* 26 (2000) 685.
22. A.-M. Azad, T.Y. Pang, M.A. Alim, *Smart. Mater. Struct.* (2000) (in press).
23. A.-M. Azad, L.J. Min, *Ceram. Int.* 27 (2001) 325.
24. A.-M. Azad, L.J. Min, M.A. Alim, *Ceram. Int.* 27 (2001) 335.
25. G. Pfaff, *Thermochim Acta*, 237 (1994) 83.
26. *Smithells Metals Reference Book*, 6th ed., E.A. Brander (Ed.), Butterworths, London, 1983, pp. 11–336.
27. *Metals Handbook*, vol. 8, 8th ed., American Society for Metals, Metals Park, OH, 1973.
28. R.D. Shannon, *Inorg. Chem.* 6 (1967) 1474.
29. NBS Monograph 25 (1972) 10.
30. L.L.Y. Chang, R.C. Kaldon, *J. Am. Ceram. Soc.* 59 (1976) 275.
31. A.-M. Azad, L.J. Min, in: M. A. Khan, A. Haq, K. Hussain, A. Q. Khan (Eds.), *Proceedings of the 6th International Symposium on Advanced Materials*, Dr. A. Q. Khan Research Laboratories, Kahuta, Pakistan, 1999, pp.32–36.
32. W.F. Smith, *Principles of Materials Science and Engineering*, 3rd Ed., McGraw-Hill, Inc., New York, 1996, pp. 560.